Post-Earthquake Capacity Evaluation of R/C Buildings based on Pseudo-Dynamic Tests

Masaki MAEDA[1]

Daeeon KANG[2]

ABSTRACT

In this paper, Post-earthquake capacity evaluation method of reinforced concrete buildings was studied. Substructure pseudo-dynamic test and static loading test of first story column in a four-story R/C building was carried out in order to investigate the validity of the evaluation method proposed by authors. In pseudo-dynamic test, different levels of damage were induced in the specimens by pre-loading, and input levels of seismic motion, at which the specimens reached to the ultimate stage, were examined. From the experimental result, no significant difference in damage levels such as residual crack width between the specimens under static and pseudo-dynamic loading was found. It is shown that residual seismic capacity ratio η proposed by authors can provide a reasonable estimation of post-earthquake seismic capacity of R/C buildings suffered earthquakes.

1. INTRODUCTION

In damage investigation of building structures suffering from earthquake, estimation of residual seismic capacity is essential in order to access the safety of the building against aftershocks and to judge the necessity of repair and restoration. The authors have proposed an evaluation method for post-earthquake seismic capacity of reinforced concrete (R/C) buildings based on the residual energy dissipation capacity of structural members [Bunno and Maeda, 2000]. The proposed method was adopted in the Japanese "Damage Level Classification Standard" revised in 2001 [JBDPA, 2001].

In this paper, substructure pseudo-dynamic test of first story column in a four-story R/C building was carried out in order to investigate the validity of the proposed evaluation method for post-earthquake seismic capacity. In pseudo-dynamic test, different levels of damage were induced in the specimens by pre-loading, and input levels of seismic motion, at which the specimens reached to the ultimate stage, were examined. Evaluation method for post-earthquake seismic capacity was discussed based on the test results.

[1] *Department of Architecture and Building Science, Tohoku University, Sendai, Japan*
Email: maeda@struct.archi.tohoku.ac.jp
[2] *Department of Architecture and Building Science, Tohoku University, Sendai, Japan*
Email: kde0898@struct.archi.tohoku.ac.jp

2. OUTLINES OF EXPERIMENT

2.1 Description of Specimens

Four column specimens were tested in this study. The specimen represented an interior column in the first story of an existing 4-storied R/C building as shown in Figure 1. All specimens have the same dimension and reinforcement. The properties and reinforcing details are shown in Figure 2 and Table 1. The dimensions of a column section were 40 x 50 cm and shear span-to-depth ratio was 1.5 (150cm height). Ten D19 bars (nominal diameter of 1.91cm, nominal area of 2.87cm^2) were arranged as longitudinal reinforcement. 19ϕ bars (round bar, diameter of 1.9cm) were arranged as lateral reinforcement with 12.5cm spacing. Mechanical properties of concrete and reinforcement are shown in Table 2.

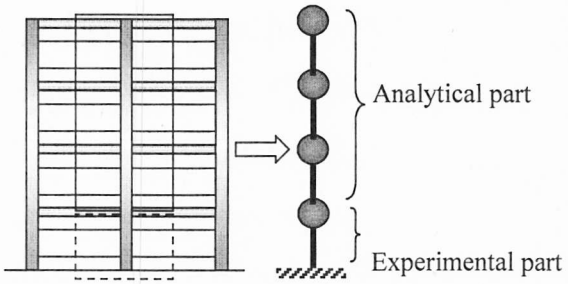

Figure 1: Objective building and analytical model for pseudo-dynamic test

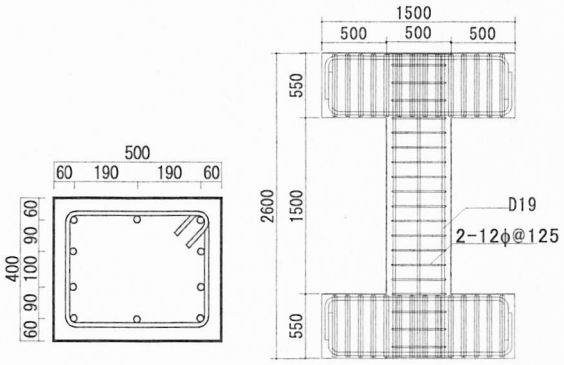

Figure 2: Dimensions and reinforcements distribution of specimens

Table 1: Dimensions and reinforcements of specimens

$B\times D$	h_0	Longitudinal Reinforcement	p_t	Shear Reinforcement	p_w	N
400×500	1500	10−D19	0.57	2−12 ϕ @125	0.45	953

h_0 : clear height (mm), p_t : tension reinf. ratio(%), p_w : lateral reinf. ratio(%), N : axial load(kN)

Table 2: Material properties of concrete and reinforcements

Concrete		Reinforcements		
σ_y (Mpa)	ε_{cu} (%)	Size and Quality	σ_y (Mpa)	ε_y (%)
27.2	0.18	D19	364	0.187
		12 ϕ	329	0.161

σ_y :Compressive Strength, ε_{cu} :Strain at the Strength σ_y :Yield Strength, ε_y :Yield Strain

2.2 Parameters of Experiment

Experimental parameters are shown in Table 3. Three specimens named PSD0, PSD2, and PSD3 were examined by pseudo-dynamic testing. The specimens PSD2 and PSD3 were damaged by pre-loadings. Target initial damage levels for PSD2 and PSD3 were minor damage (damage class II by the Damage Level Classification Standard, see Table 4) and moderate damage (damage class III), respectively. On the other hand, PSD0 was tested with no structural damage. The damaged and undamaged specimens were tested by pseudo-dynamic testing using amplified input seismic motion at which the specimens reached to the ultimate stage. The specimen ST was tested by static loading to compare the failure patterns, damage levels and hysterisis loops with the specimens under pseudo-dynamic testing.

Table 3: Parameters of experiment

	Loading	Initial damage	Damage class*
PSD0	Pseudo-Dynamic	None	0
PSD2		Minor	II
PSD3		Moderate (or Severe)	III
ST	Static	None	0

* Damage Level Classification Standard [JBPDA, 2001]

Table 4: Damage classification of structural members [JBPDA, 2001]

Damage class	Observed damage on structural members
I	Some cracks are found. Crack width is smaller than 0.2 mm.
II	Cracks of 0.2 - 1 mm wide are found.
III	Heavy cracks of 1 - 2 mm wide are found. Some spalling of concrete is observed.
IV	Many heavy cracks are found. Crack width is larger than 2 mm. Reinforcing bars are exposed due to spalling of the covering concrete.
V	Buckling of reinforcement, crushing of concrete and vertical deformation of columns and/or shear walls are found. Side-sway, subsidence of upper floors, and/or fracture of reinforcing bars are observed in some cases.

2.3 Test Method and Loading System

2.3.1 Loading apparatus

Loading apparatus is illustrated in Figure 3. The specimens were subjected to bending and shear by a horizontal jack. The vertical jacks on both side of the specimen kept the top and

bottom stubs and applied constant axial. The specimen ST was subjected to two cycles at drift angle of 1/200, 1/100, 1/67, 1/50, 1/33 rad. after the first cycle at a drift angle of 1/400.

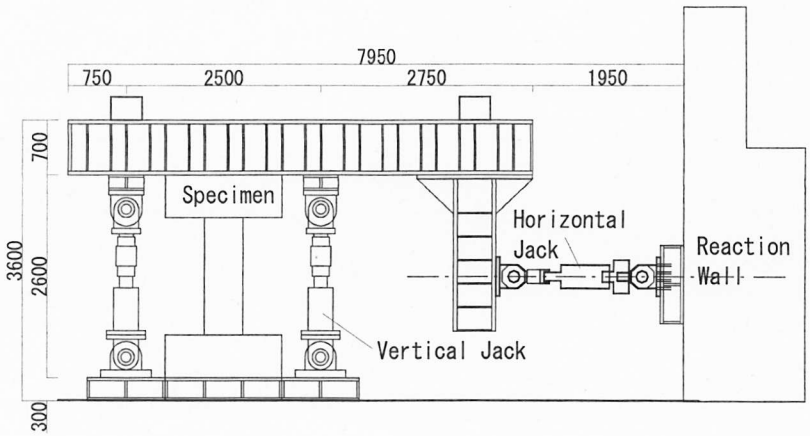

Figure 3: Testing apparatus

2.3.2 Method of Pseudo-Dynamic Test

The specimens PSD0, PSD2 and PSD3 were tested by sub-structure pseudo-dynamic method. The objected building was reduced to a 4-degree-of-freedom system. As shown in Figure 1, the column specimen represents the first story column and second to fourth stories were analyzed. The specimen was subjected to the target story drift angle which was calculated from step-by-step seismic response analysis of the 4-degree-of-freedom system. Takeda model was used as hysteresis model for the analytical parts in seismic response analyses. The crack and yielding strengths of the specimens are calculated according to the Japanese "Standard for Structural Calculation" [AIJ, 1999]. Time increment of response analysis was 0.005 second and OS-method [Nakajima et al., 1990] was applied to numerical integration. Viscous damping matrix was assumed to be proportional to stiffness matrix at yielding, which was 2% of natural frequency.

NS component of JMA (Japan Meteorological agency) KOBE recorded at 1995 Hyogo-ken-nambu Earthquake was adopted for the input ground motion. The input acceleration is shown in Figure 4. Table 5 shows the target structural damage levels of the specimens and the amplification factors of input ground acceleration for each RUNs, respectively. As mentioned earlier, specimens PSD2 and PSD3 were induced structural damage of damage class II and III, respectively, by pre-loading named "RUN0" in order to estimate the residual seismic capacity. Note that additional pre-loading "RUN0+" was applied to specimen PSD2 because the damage level due to the RUN0 remained damage class I. Then all specimens were subjected to amplified input acceleration so that the specimen reached to the ultimate state and failed (damage class V).

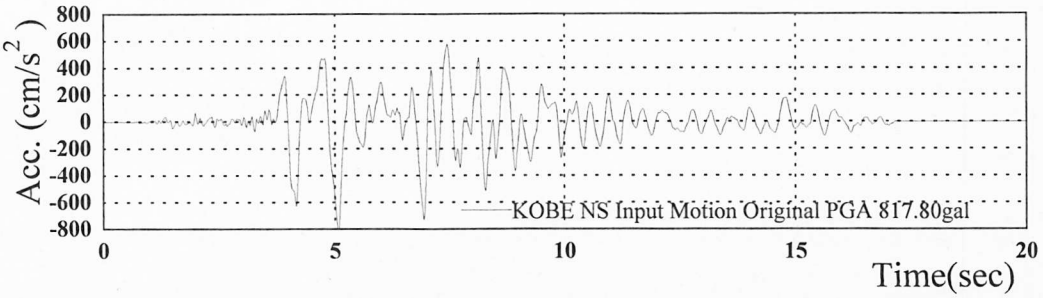

Figure 4: Acceleration record for input ground motion (JMA Kobe NS)

Table 5: Target structural damage and amplification factor of input acceleration

Specimen	Input	Target Damage Level	Amplification Factor
PSD2	RUN0	II	0.25
	RUN0$^+$		0.41
	RUN1	V	0.41
PSD3	RUN0	III	0.50
	RUN1	V	0.30
PSD5	RUN1	V	0.60

3. TEST RESULTS

3.1 Results of Static Loading

Figure 5 shows the observed shear force – lateral displacement relation for specimen ST. Crack pattern was shown in Photo 1. Longitudinal bars yielded at the drift angle of the order of 1/200 after generation of flexural and shear cracks. The process to failure was as follows; i.e., at a drift angle of 1/100rad., bond splitting cracks along longitudinal bars were observed. The lateral load began to decrease gradually with propagation of bond splitting cracks and, finally, bond splitting failure was observed.

The relationship between the maximum residual crack width and drift angle at the peak of each cycle was shown in Figure 6. The residual crack widths were measured by crack scale at the moment when the lateral force was unloaded. In the figure, crack width of 0.2, 1, and 2mm correspond to the borders between the damage classes of the structural members, according to Table 4 [JBDPA 2001]. The crack widths were smaller than 0.2mm, which correspond to the "damage class I (slight damage)", until flexural yielding occurred in a cycle at 1/200rad. After flexural yielding, the maximum residual crack widths increased markedly with increase in drift angle.

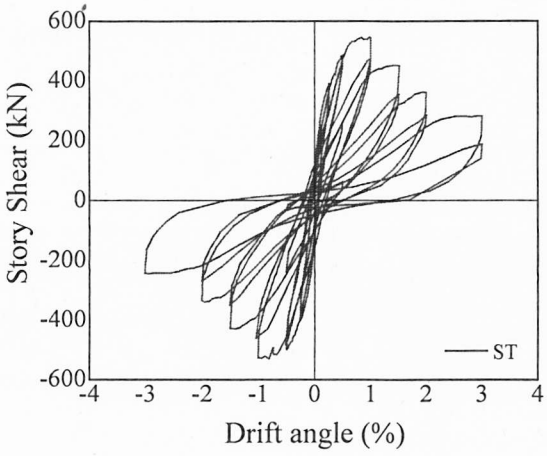

Figure 5: Story shear vs. drift angle

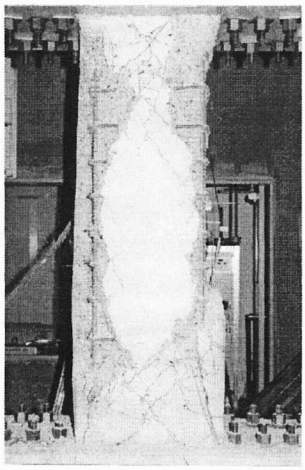

Photo 1: Crack patterns at the final cycle

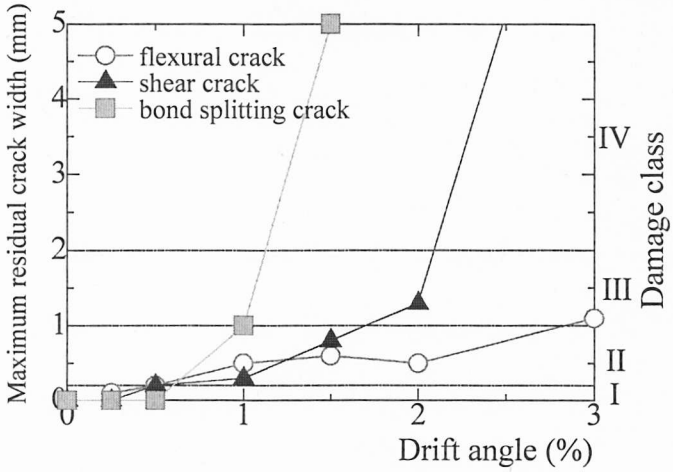

Figure 6: Maximum crack width vs. drift angle

3.2 Results of Pseudo-dynamic Loading

Figure 7 shows the observed shear force – lateral displacement relations of specimen PSD0, PSD2 and PSD3. The relationship between the maximum residual crack width and drift angle at the peak of each cycle was shown in Figure 8. Crack patterns after the pre-loading, RUN0, were shown in Photo 2.

The process to failure was almost similar to the specimens ST. In specimen PSD0 which was subjected to 0.60 time JMA Kobe NS record, after flexural yielding was observed at drift angle of 0.61%, shear force began to decrease with propagation bond splitting cracks and the specimen failed.

Maximum drift angle was 0.5% and maximum residual crack widths was 0.2mm (damage class I) in RUN0 of specimen PSD2, in which amplification factor for the input acceleration was 0.25. In the RUN0^{+} (amplification factor was 0.41), after the specimen yielded at the drift angle of 0.61% and maximum drift angle reached to 1.0% with maximum residual crack

width of 0.5mm (damage class II). In the RUN1 (amplification factor was 0.41), the specimen failed in bond splitting due to rapid increase in drift angle.

Maximum drift angle of 2.24% and bond splitting crack of 3.5mm width, which was somewhat larger than the criteria of the target damage class III were induced by the RUN0 of specimen PSD3 (amplification factor was 0.50). In the RUN1 with amplification factor of 0.30, shear resistance was deteriorated gradually due to bond splitting failure, although maximum drift angle did not increase markedly.

As can be seen from Figure 8, no significant difference in residual crack widths between the specimens under static and pseudo-dynamic loading was found.

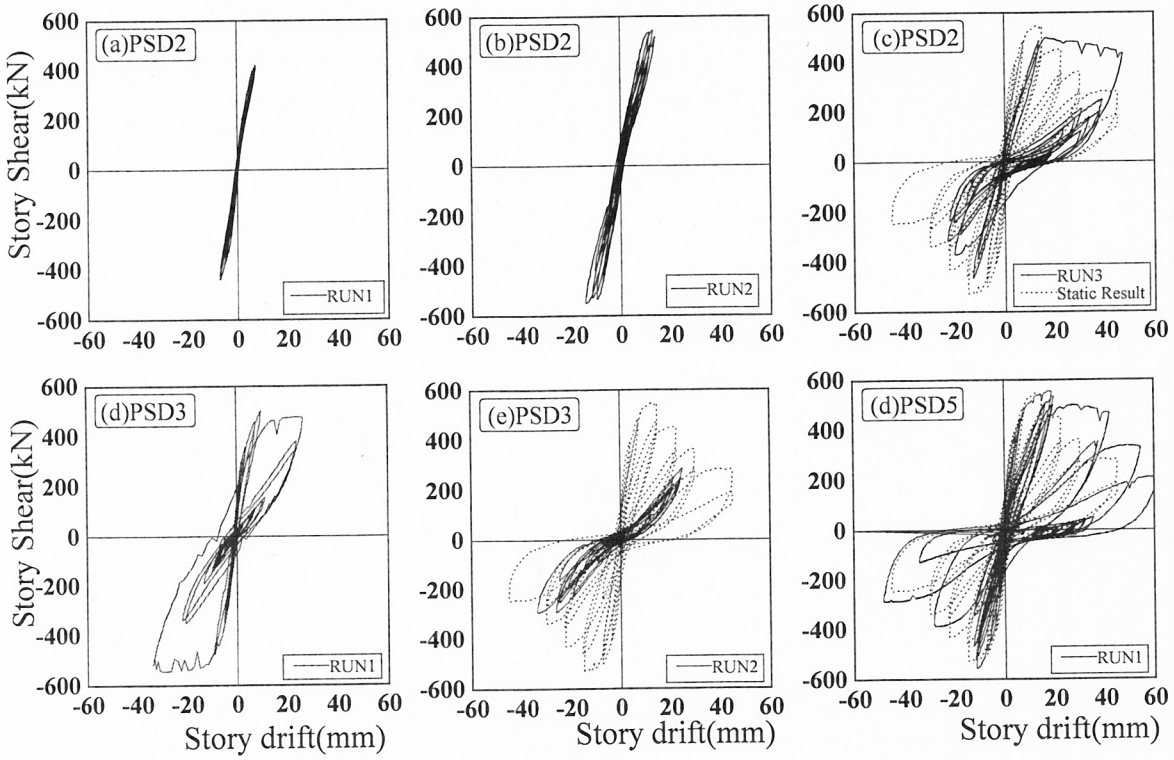

Figure 7: Relationships between story shear and drift angle

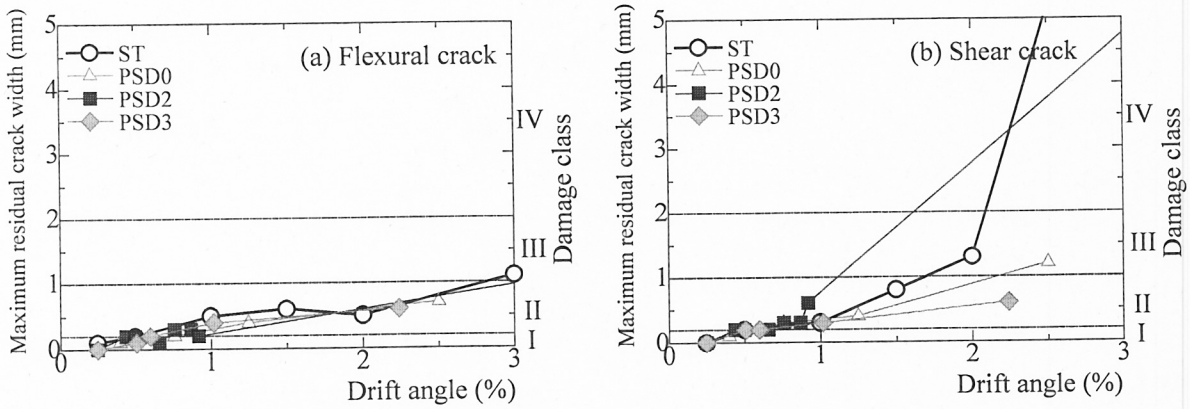

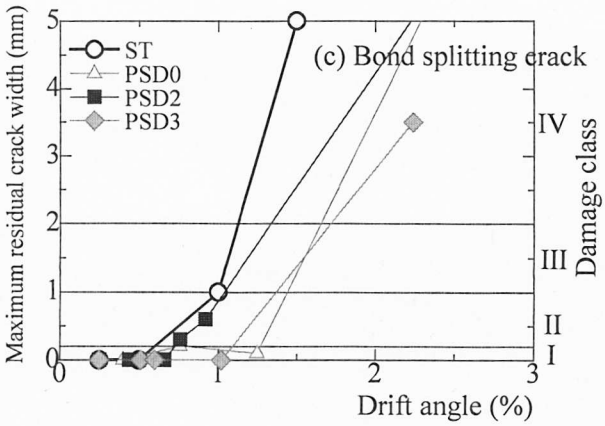

Figure 8: Maximum residual crack width vs. drift angle

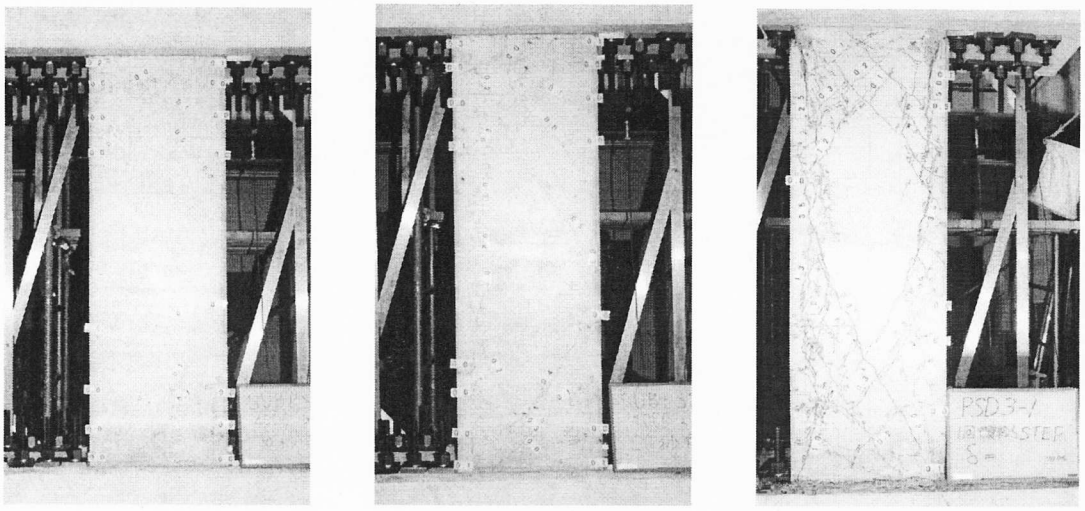

(a) RUN0 of PSD2 **(b) RUN0^{+} of PSD2** **(c) RUN0 of PSD3**

Photo 2: Crack patterns after pre-loading

The relationships between the amplification factor of input acceleration and maximum ductility factors are shown in Figure 9. In the figure, the lines indicate analytical results for the first story of the 4-degree-of-freedom system and the marks are experimental results. Figure 9(a) indicates the results without structural damage; i.e., RUN1 for PSD0 and RUN0 for PSD2 and PSD3. Figure 9(b), (c) and (d) indicate the results after pre-loading. From the figure, maximum ductility response increases with increase in amplification factor of input ground motion. The maximum ductility responses after some damage was induced (Figure 9(b), (c) and (d)) are generally larger than those without damage. Experimental results approximately agreed well with the analytical results although disagreement can be found for the results of ductility factor of larger than 5 because pinching behavior and deterioration of shear resistance were not taken into account in the hysteresis model for the analyses.

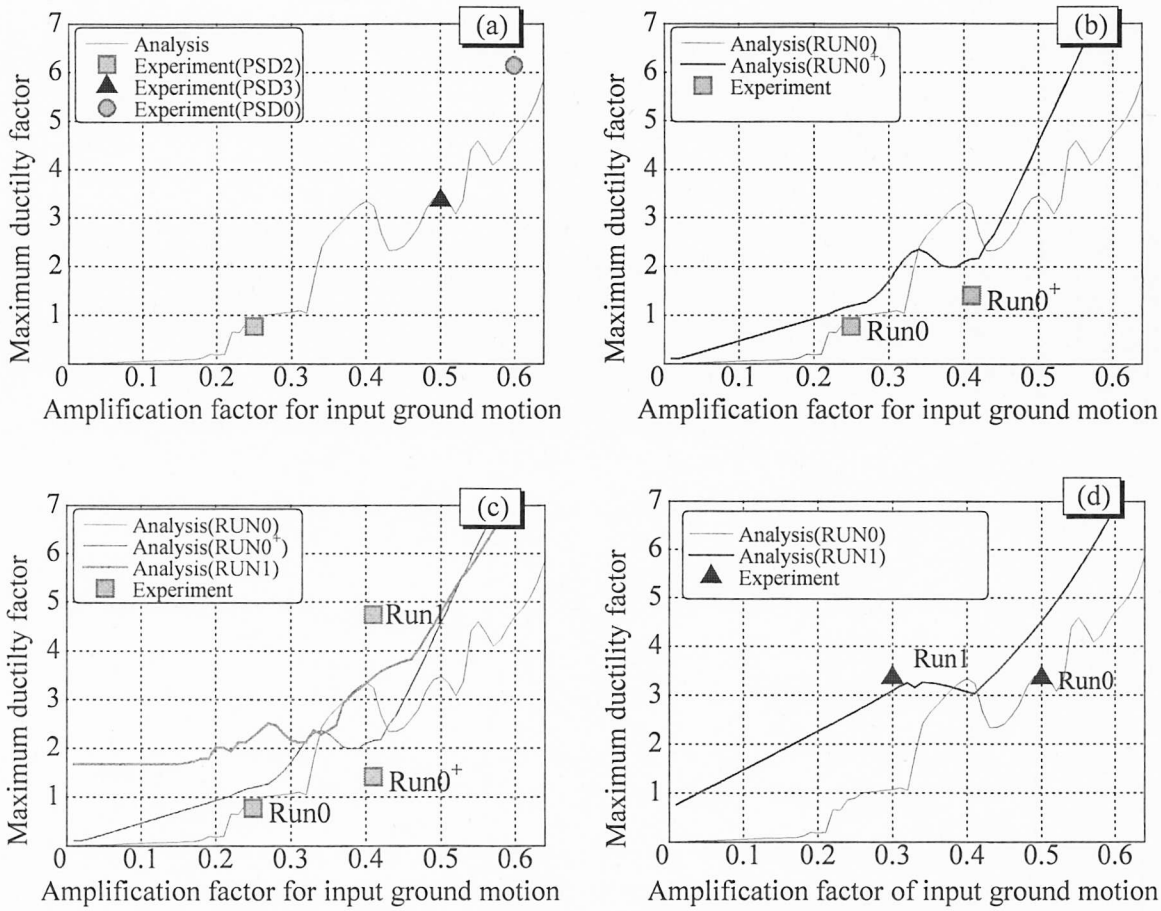

Figure 9: Relationship between amplification factor of input ground motion and maximum ductility factor

4. ESTIMATION OF RESIDUAL SEISMIC CAPACITY

The authors evaluated residual seismic capacity ratio η of structural members for each damage class as shown in Table 6 based on experimental data of beams and columns under static loading. The basic concept of residual seismic capacity ratio η is illustrated in Figure 10. Deterioration of seismic capacity was estimated by energy dissipation capacity in lateral force- displacement curve of each member. The residual seismic capacity ratio η was defined as the ratio of residual energy dissipation capacity to the total capacity and given by Eq.(1).

$$\eta = \frac{E_r}{E_t} \tag{1}$$

where, E_d: dissipated energy, E_r: residual energy capacity, E_t: entire energy capacity ($E_t = E_d + E_r$).

Table 6: Residual seismic capacity ratio η

Damage class	Brittle members	Ductile members
I	0.95	0.95
II	0.6	0.75
III	0.3	0.5
IV	0.0	0.1
V	0.0	0.0

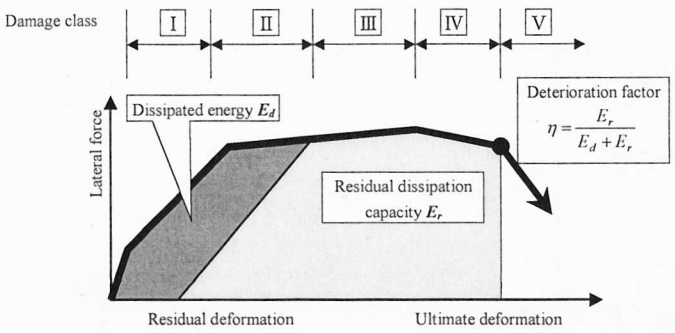

Figure 10: Seismic capacity reduction factor η

To investigate the validity of the proposed residual seismic capacity ratio η, input ground motion levels with which the specimen failed in the pseudo-dynamic testing were compared with residual seismic capacity ratio η in Figure 11. In the figure, thick line and broken line indicate residual seismic capacity ratio η for brittle and ductile members respectively. The circles indicate amplification factors of input acceleration in the pseudo-dynamic testing. Amplification factor of 0.60 for undamaged specimen PSD0 was assumed to correspond to the original capacity, η=1.0. As can be seen from the figure, amplification factor of 0.41 for RUN1 of PSD2 and 0.30 for RUN1 of PSD3 approximately correspond to the residual seismic capacity ratio η. Accordingly, the proposed residual seismic capacity ratio η might be useful for the reasonable estimation of post-earthquake seismic capacity of damaged R/C buildings.

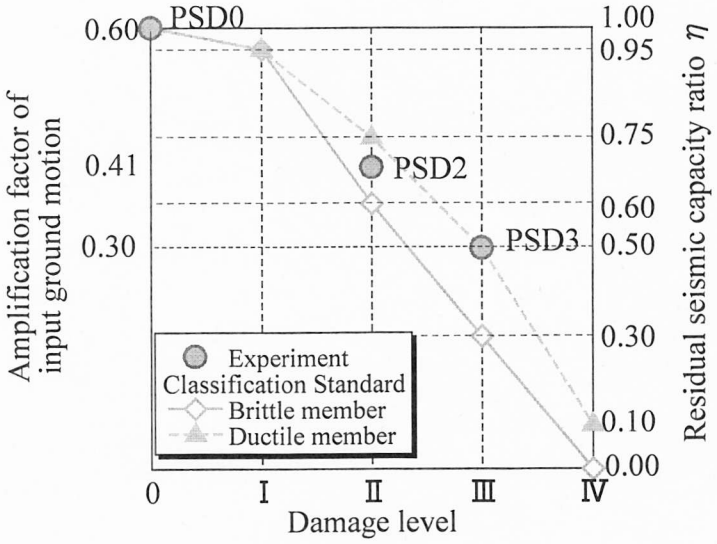

Figure 11: Comparison of seismic capacity reduction factor η with amplification factor of input ground motion

6. CONCLUSIONS

In this paper, static loading test and sub-structural pseudo-dynamic test of R/C columns were carried out to investigate the validity of the method for post-earthquake capacity evaluation proposed by the authors. From the experimental result, no significant difference in damage levels such as residual crack width between the specimens under static and pseudo-dynamic loading was found. It is shown that residual seismic capacity ratio η proposed by the authors can provide a reasonable estimation of post-earthquake seismic capacity of R/C buildings suffered earthquakes.

7. REFERENCES

AIJ / Architectural Institute of Japan (1999), *Standard for structural calculation of reinforced concrete structure*. (in Japanese)

Bunno, M., Maeda, M., and Nagata, M. (2000), "Damage level classification of reinforced concrete buildings based on member residual seismic performance (in Japanese)", *Proceedings of the Japan Concrete Institute*, Vol. 22, No. 3, JCI, pp.1447-1452.

Bunno, M., Nagayama, K., Maeda, M., and Tasai, A. (2001), "An evaluation of residual seismic capacity of reinforced concrete columns based on structural damage (in Japanese)", *Proceedings of the Japan Concrete Institute*, Vol. 23, No. 3, JCI, pp.259-264.

JBDPA / The Japan Building Disaster Prevention Association (2001), *Standard for Damage Level Classification of Reinforced Concrete Buildings*. (in Japanese)

Jung, M., Maeda, M., Tasai, A. and Nagata, M. (2001), "Relationship between residual seismic performance and damage level on seismic response of reinforced concrete buildings (in Japanese)", *Proceedings of the Japan Concrete Institute*, Vol. 23, No. 3, JCI, pp.1219-1224.

Nakajima, M., Ishida, M., and Ando, K (1990), "Integration Techniques for Substructure Pseudo Dynamic Test (Pseudo dynamic test using substructuring techniques) (in Japanese)", *Journal of structural and construction engineering, Transaction of AIJ*, No.417, pp.107-118,